

## NUMERICAL AND EXPERIMENTAL STUDIES OF PARTICLE ACCELERATION

### POWERED BY MODULATED INTENSE RELATIVISTIC ELECTRON BEAMS

J. Krall\*, M. Friedman, V. Serlin and Y.Y. Lau  
 Plasma Physics Division  
 Naval Research Laboratory  
 Washington, DC 20375-5000

\*Science Applications Intl. Corp.  
 McLean, VA 22102

**Abstract:** A fully electromagnetic particle code is used to simulate the transfer of energy from an annular modulated intense relativistic electron beam to a secondary low current electron beam via a disk-loaded structure. It is shown that the modulated intense beam can be used to drive such an accelerator at a high transformer ratio ( $R \approx 10$ ) with an accelerating gradient in the  $\sim 100$  MV/m range. Power in excess of 1 GW was transferred from the primary to the secondary beam. An experiment was performed in which such a beam (diameter 13 cm, peak power 8 GW) dumped RF power into a disk-loaded structure of length one meter. This RF power was transferred from the structure to a secondary electron beam resulting in acceleration of electrons to an energy much greater than 10 MeV with current of the order 300 Amps.

#### Introduction

It has been shown that high electric fields of the order of 100 MV/m can be established in RF accelerating structures by modulated intense relativistic electron beams (MIREB's) of power greater than  $10^9$  W.<sup>1,2</sup> Novel accelerators, in which a low voltage, high current beam interacts via a metallic structure to power a low current beam to very high energies have been suggested by Voss and Weiland,<sup>3</sup> among others. Wake field acceleration has been observed in experiments by Figueroa et al.<sup>4</sup>

Accelerators powered directly by MIREB's have several advantages over conventional accelerators:<sup>2,5</sup>

(1) Previous results<sup>5</sup> suggest that the high RF power of a MIREB may be coupled to an RF structure so as to drain significant power ( $> 1$  GW) from the beam at high efficiency.

(2) Geometrical effects may allow for sizeable variations in efficiency, field gradient, and coupling between the MIREB and the RF structure.

In the present paper we study these issues via an axisymmetric particle simulation using the CONDOR<sup>6</sup> code and present preliminary experimental results.

The accelerator configuration to be studied is similar to that outlined in Ref. 2 and is pictured in Fig. 1.

(1) An IREB of radius  $r_b \approx 6.3$  cm, current  $I_0 = 16$  kA and energy  $E_{inj} = 500$  keV is injected into an evacuated drift tube of radius  $r_w = 6.8$  cm. The IREB is focussed by an axial field  $B_0 = 10$  kG throughout.

(2) The IREB is fully modulated at a frequency  $f \approx 1.3$  GHz by two tuned cavities. The first cavity is externally driven by a low level RF source (magnetron). The second cavity is undriven.

(3) The MIREB is guided into a drift tube of radius 9.6 cm. The tube contains an accelerating structure which consists of thin disks of radius 9.0 cm and separation 1.88 cm. The MIREB, which has a frequency of modulation corresponding to the desired mode of the RF structure, is terminated at the first disk. A resonant interaction occurs between the MIREB and the RF fields, extracting energy from the MIREB at the gap (defined by the end of the drift tube and the first disk of the RF structure).

(4) An emitter, located on axis on the surface of the first disk, emits a secondary beam which is accelerated by the RF fields.

Modulation of an IREB has been previously reported<sup>5,7,8</sup> and has been repeated experimentally with the present parameters.<sup>9</sup>

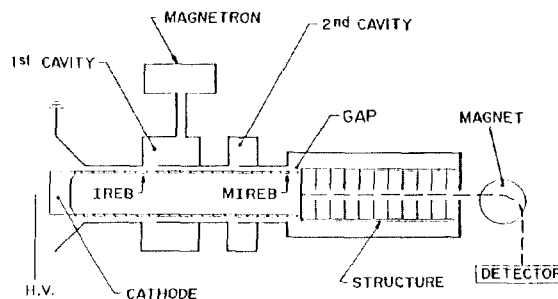


Fig. 1. MIREB-driven accelerator schematic.

#### Fields in the RF Structure

The interaction between the primary and secondary beams in this accelerator is different than the wake field schemes of Refs. 3 and 4, where the two beams travel colinearly. Here, the interaction of the primary beam with the RF structure takes place only as the beam traverses the gap, while the secondary beam is accelerated along the entire length of the RF structure. The transformer ratio is defined as

$$R = \frac{\langle E_{axis} \rangle L}{E_{gap} d}, \quad (1)$$

where  $d$  is the gap length,  $L$  is RF structure length,  $E_{gap}$  is the gap field and  $\langle E_{axis} \rangle$  is the average field experienced by the accelerated particles.

The normal modes of the RF structure can be solved for by neglecting the interaction region at the gap.<sup>2</sup> Here, we consider the only fundamental mode of a disk-loaded cavity of length  $L = n\lambda/2$  where  $\lambda$  is the wavelength of the RF and  $n$  is a positive integer. The  $z$ -component of the electric field of the fundamental mode varies sinusoidally along the axis and radially as

$$E_z(r)/E_z(r=0) = J_0(kr)/J_0(kr_0), \quad (2)$$

where  $J_0$  is a Bessel function and  $k = 2\pi/\lambda$ . It was conjectured in Ref. 2 that the ratio of the field experienced at the gap by the primary beam to the peak field on axis would follow this radial variation so that  $E_{axis}/E_{gap} \approx 1/J(kr_b)$ .

The normal modes for a given axisymmetric cavity may be calculated numerically by using the Superfish<sup>10</sup> code. Superfish calculations have been performed for a disk-loaded cavity of length  $L \approx \lambda$  with the gap region included. A series of such calculations showed that the expected cavity mode was obtained.<sup>11</sup>

The nonaxisymmetric modes for this structure have also been studied to show that beam breakup growth due to such modes is benign for the parameters of the present proof-of-principle experiment.<sup>12</sup>

### Numerical Simulations

The simulation geometry (Fig. 2) consisted of a short drift tube region with radius  $r_w = 6.8$  cm, a gap of length  $d = 1.57$  cm and a disk-loaded structure of length  $L = 22.2$  cm  $\approx \lambda$ , where  $\lambda = c/f$ , and  $f = 1.27$  GHz is the frequency of the accelerating mode of the cavity, and was determined numerically.

The primary beam was injected from the left-hand wall with radius  $r_b = 6.4$  cm, energy  $E_{inj} = 2.0$  MeV and current  $I_{inj}(kA) = g(t)[16 + 8\sin(2\pi ft)]$ , where  $g(t)$  is an envelope function that increases linearly from zero to unity during the time  $0 < t < 15$  ns and remains constant thereafter. At  $t = 17$  ns, the secondary beam with  $I_2 = 10$  Amps and  $E_2 = 0.1$  MeV was injected continuously from the center of the first disk and was accelerated along the axis by the RF fields. The simulation continued until  $t = 30$  ns.

Note that in order for this structure to behave like a cavity, the parameters  $L$ ,  $v_g$  and  $T$  must be such that  $L/v_g \ll T$ , where  $v_g$  is the group velocity of E-M radiation within the disk-loaded structure and  $T$  is the duration of the primary beam pulse. In the geometry of Fig. 2,  $v_g/c$  is a sizable fraction of unity, satisfying this constraint within the 30 ns duration of the simulation.

Several differences between this configuration and that of an experiment must be noted.

(1) In an experiment the disk structure would be longer so as to obtain a higher energy secondary beam.

(2) An actual device would have support rods to hold the disks in place, providing a DC current path for the primary beam. Because such supports cannot be modelled in two dimensions, we added a center conductor between the first disk and the left-hand boundary (ground). This did not significantly effect the results.<sup>11</sup>

(3) In the simulation geometry, the left-hand boundary was a metallic wall. In reality, this boundary is an open drift tube, for which symmetric RF modes at a frequency of 1.27 GHz are below cutoff.

(4) The simulation structures were defined on a grid such that the effective skin depth of the material is one grid cell ( $\Delta r = 0.2$  cm,  $\Delta z = 0.3133$  cm), making the cavity extremely lossy, with  $Q$  of order 10. A typical value for the experimental structure is of order 1000.

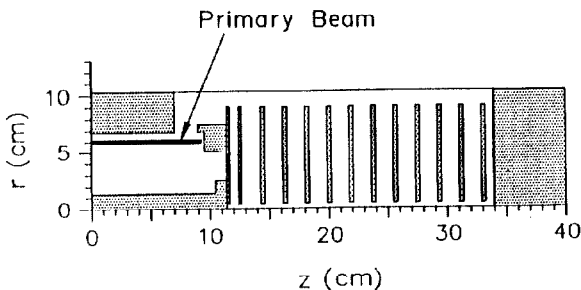


Fig. 2. Simulation geometry. The secondary beam is injected on axis at  $z \approx 12$  cm.

Figure 3 shows the  $z$ -component of the electric field plotted versus time in the gap and on the axis of the RF structure. These fields increased continuously, reaching values of 56.3 MV/m at the gap and 94.2 MV/m on axis before the simulation was

halted. The plot of the gap electric field shows evidence of a weak, lower frequency mode which may have been excited by the increase in DC current from  $t = 0$  to  $t = 15$  ns. The RF cavity mode, as expected, was a standing wave, varying sinusoidally in  $z$  and radially as a Bessel function,  $J_0(kr)$ .

The acceleration of the secondary beam can be seen in Fig. 4. Here, particle positions were plotted in phase space,  $\gamma\beta c$  vs.  $z$ , where  $\beta$  is the axial particle velocity normalized to  $c$  and  $\gamma = (1 - \beta^2)^{-1/2}$ . The particle positions, plotted at fixed time at intervals of 0.2 ns, show a maximum energy increase of 8.60 MeV over 22.2 cm to give an accelerating gradient of 39.2 MV/m. With this result and the observed 56.3 MV/m at the gap, a transformer ratio  $R = 9.85$  has been achieved.

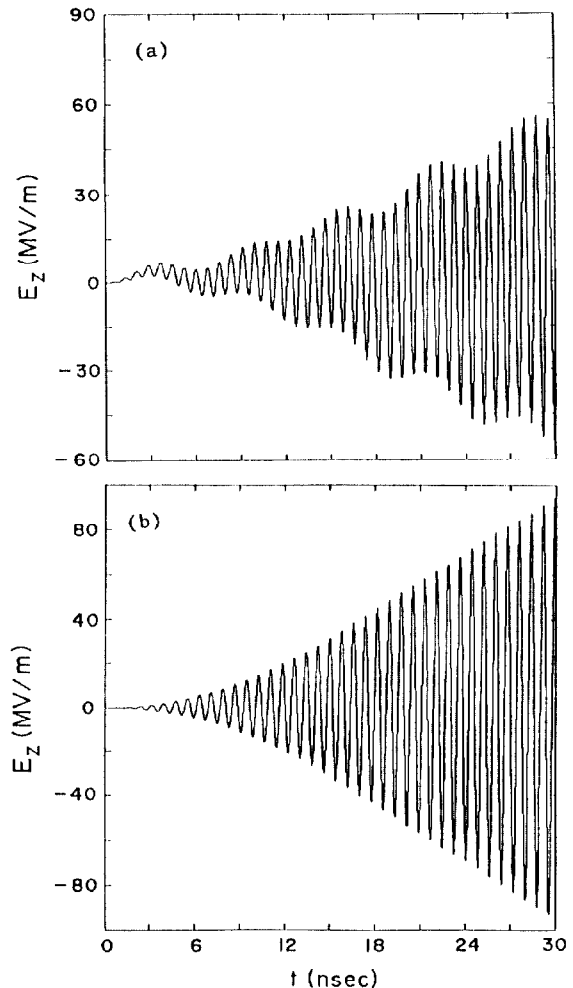


Fig. 3.  $E_z$  versus time at the gap and on axis (at peak field) for the  $r_b = 6.4$  cm case.

Several interesting aspects of this simulation should be noted.

(1) The build-up of RF in the cavity was of a transient nature. Were the simulation not halted at  $t = 30$  ns, the field amplitudes would increase beyond the observed 94.2 MV/m. Realistically, limitations may include breakdown in the RF structure, low  $Q$ , termination of the primary beam, or loading due to high current in the secondary beam.

(2) The conjectured relationship between  $r_b$  and  $E_{axis}/E_{gap}$ , discussed in connection with Eq. (2) above, did not hold. Here, we have  $E_{axis}/E_{gap} = 1.67$  and  $1/J_0(kr_b) = 2.51$ . The effect of varying  $r_b$  will be investigated below.

(3) The electric field of 56.3 MV/m that was observed across the 1.57 cm gap indicates that the primary beam loses 0.883 MV as it traverses the gap. This energy loss is verified by the phase-space plots of Fig. 4, where the primary beam particles, which have  $0 < z < 10$  cm, were deflected in momentum space by the gap voltage. This indicates a power drain of 7.07 GW at 1.27 GHz and is sufficient power to accelerate secondary beam current in the 500 Amp range over this short distance. With a longer accelerating structure, lower currents may be accelerated to higher energies.

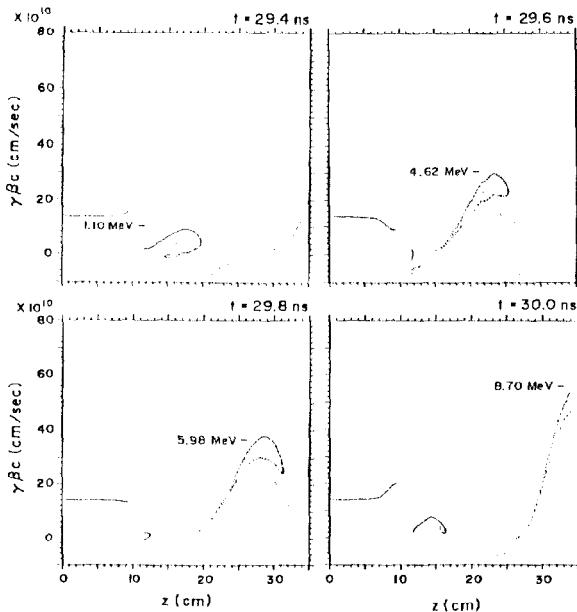


Fig. 4. Particle positions in phase-space,  $y\beta_{zc}$  versus  $z$ , at intervals of 0.2 ns. The primary beam is on the left,  $0 < z < 10$  cm. The peak energy of the accelerating secondary beam particles is noted.

The simulation of Figs. 3 and 4 was repeated with 200 Amps secondary beam current. We found  $E_{\text{gap}} = 51.6$  MV/m,  $E_{\text{axis}} = 91.3$  MV/m,  $\langle E_{\text{axis}} \rangle = 35.7$  MV/m and  $R = 9.78$ . We obtained secondary beam RF power of 1.58 GW without significantly loading the cavity.

The effect of varying  $r_b$  was investigated by repeating the simulation of Figs. 3 and 4 with  $r_b = 8.0$  cm, necessitating an increase in the drift tube radius to  $r_w = 8.4$  cm. This shifted the resonance slightly, to 1.34 GHz. We have obtained the following results:

(1) We found  $E_{\text{gap}} = 13.5$  MV/m,  $E_{\text{axis}} = 34.4$  MV/m and  $\langle E_{\text{axis}} \rangle = 14.3$  MV/m.  $R$  was increased to 15.0.

(2) With  $r_b = 8.0$ , we have  $E_{\text{axis}}/E_{\text{gap}} = 2.55$  and  $1/J_0(kr_b) = 11.9$ . The conjectured relation between  $r_b$  and  $E_{\text{axis}}/E_{\text{gap}}$  held only in a qualitative sense.

(3) The fields in the cavity reached much lower amplitudes at  $t = 30$  ns than in the  $r_b = 6.4$  cm case, indicating a weakening of the interaction between the primary beam and the RF structure.

(4) The mode structure was unchanged from the previous case. Note that at  $r_w = 8.4$  cm,  $f = 1.34$  GHz is very close to the cutoff frequency  $f_c = 1.37$  GHz. Realistically, it may not be possible to increase  $r_b$  and  $r_w$  to such values at this frequency.

## Experimental Results

An experiment has been performed in which a 13 cm diameter annular IREB of DC current 16 kA and voltage 500 kV was fully modulated at a frequency of 1.328 GHz. The modulated electron beam was terminated in such a way that the RF energy was transferred into the disk-loaded structure as in Fig. 1. A cold emission cathode was placed at the center of the first disk. The electron beam emitted from this cathode had a diameter of 1 mm and current of 300 Amps. This electron beam propagated along the length of the structure (1 meter) without loss of current or radial expansion.

Preliminary diagnostics based on the stopping range of the accelerated electrons in absorbers indicate that electrons with energy much greater than 10 MeV were present. More sophisticated diagnostics are currently being designed.

## Conclusions

We have demonstrated that high fields and transformer ratios can be supported by a MIREB-driven accelerator, with power in excess of 1 GW transferred from the primary to the secondary beam, despite the low  $Q$  of the numerical structure.

We have found that the build-up of RF fields in the structure is transient by nature with peak accelerating gradients limited only by the brevity of the simulations. In an actual device, field amplitudes will continue to increase until limited by such mechanisms as saturation (low  $Q$ ) or termination of the primary beam pulse.

We have also shown that by varying the primary beam radius, the transformer ratio may be increased, but at the cost of weakening the coupling between the primary beam and the RF structure.

Finally, in a preliminary experiment electrons were accelerated to energies in excess of 10 MeV and with peak current of 300 Amps.

## Acknowledgement

This work was supported by the Department of Energy under contract number DE-AI05-86-ER13585.

## References

1. M. Friedman and V. Serlin, Phys. Rev. Lett. **55**, 2860 (1985).
2. M. Friedman and V. Serlin, Appl. Phys. Lett. **49**, 596 (1986).
3. G. Voss and T. Weiland, Desy Report M82-10 and Desy Report M82079, 1982.
4. H. Figueroa, W. Gai, R. Konecny, J. Norem, A. Ruggiero, P. Schoessow and J. Simpson, Phys. Rev. Lett. **60**, 2144 (1988).
5. M. Friedman, J. Krall, Y.Y. Lau and V. Serlin, J. Appl. Phys. **64**, 3353 (1988).
6. CONDOR is an extension of the MASK particle code, discussed in A. Palevsky and A. Drobot, in Proceedings of the 9th Conference on Numerical Simulation of Plasmas, July 1980 (Northwestern University, Evanston, IL) (unpublished).
7. J. Krall and Y.Y. Lau, Appl. Phys. Lett. **52**, 431 (1988).
8. Y.Y. Lau, J. Krall, M. Friedman and V. Serlin, IEEE Trans. Plas. Sci. **16-2**, 249 (1988).
9. M. Friedman, V. Serlin, Y.Y. Lau and J. Krall, to be published.
10. K. H. Halbach and R. F. Holsinger, LBL report LBL-5040, 1976.
11. J. Krall, V. Serlin, M. Friedman and Y.Y. Lau, to be published.
12. Y.Y. Lau, Bull. Am. Phys. Soc. **33**, 2040 (1988), Also in these proceedings.